

Review

# Subunit movements in membrane-integrated EF<sub>0</sub>F<sub>1</sub> during ATP synthesis detected by single-molecule spectroscopy

Boris Zimmermann<sup>a</sup>, Manuel Diez<sup>a</sup>, Michael Börsch<sup>b</sup>, Peter Gräber<sup>a,\*</sup>

<sup>a</sup> Albert-Ludwigs-Universität Freiburg, Institut für Physikalische Chemie, Albertstrasse 23a, D-79104 Freiburg, Germany

<sup>b</sup> 3. Physikalisches Institut, Universität Stuttgart, Pfaffenwaldring 57, 70569 Stuttgart, Germany

Received 13 January 2006; received in revised form 28 March 2006; accepted 28 March 2006

Available online 24 April 2006

## Abstract

The H<sup>+</sup>-ATPsynthase from *E. coli* was isolated and labelled at the  $\gamma$ - or  $\epsilon$ -subunit with tetramethylrhodamine, and at the b-subunits with bisCy5. The double labelled enzymes were incorporated into liposomes. They showed ATP hydrolysis activity, and, after energization of the membrane by  $\Delta\text{pH}$  and  $\Delta\phi$ , also ATP synthesis activity was observed. Fluorescence resonance energy transfer (FRET) was used to investigate the movements of either the  $\gamma$ -subunit or the  $\epsilon$ -subunit relative to the b-subunits in single membrane-integrated enzymes. The results show that during catalysis, the  $\gamma$ - $\epsilon$  complex rotates stepwise relative to the b-subunit. The direction of rotation during ATP synthesis is opposite to that during ATP hydrolysis. The stepwise motion is characterized by dwell times (docking time of the  $\gamma$ - $\epsilon$  complex to one  $\alpha\beta$  pair) up to several hundred ms, followed by a rapid movement of the  $\gamma$ - and  $\epsilon$ -subunit to the next  $\alpha\beta$  pair within 0.2 ms. The same FRET levels (i.e., the same  $\gamma$ -b and  $\epsilon$ -b distances) are observed during proton transport-coupled ATP hydrolysis and ATP synthesis, indicating that the reaction proceeds via the same intermediates in both directions. Under non-catalytic conditions, i.e., in the absence of ATP or without energization also, three FRET levels are found, however, the distances differ from those under catalytic conditions. We conclude that this reflects a movement of the  $\epsilon$ -subunit during active/inactive transition.

© 2006 Elsevier B.V. All rights reserved.

**Keywords:** Single-molecule spectroscopy; Fluorescence resonance energy transfer; EF<sub>0</sub>F<sub>1</sub>; Fluorescence labelling; Subunit rotation; ATPsynthase

## 1. Introduction

The H<sup>+</sup>-ATPsynthase from *E. coli*, EF<sub>0</sub>F<sub>1</sub>, couples the transmembrane proton-transport with ATP synthesis and ATP hydrolysis. The enzyme consists of a hydrophilic F<sub>1</sub> part with subunits  $\alpha_3\beta_3\gamma\delta\epsilon$ , and a hydrophobic membrane-integrated F<sub>0</sub> part with subunits  $ab_2c_{10}$  [1]. Different experimental approaches have shown that ATP hydrolysis catalyzed by isolated F<sub>1</sub> is accompanied by a rotational movement of the  $\gamma$ -subunit within the  $\alpha_3\beta_3$  barrel. Kinetic investigations have led to the “binding change” theory, where sequential docking/undocking of the  $\gamma$ -subunit to the three  $\alpha\beta$  pairs induces conformational changes in these subunits, which lead to catalysis [2]. Movement of the  $\gamma$ -subunit has been observed in F<sub>1</sub> [3,4] and F<sub>0</sub>F<sub>1</sub> [5,6]. Rotation of the  $\gamma$ -subunit in the F<sub>1</sub> part has been observed with an

ingenious single-molecule experiment using immobilized F<sub>1</sub> with a fluorescent actin filament or gold bead as an indicator of rotation [7,8]. Cross-linking of the  $\gamma$ - and  $\epsilon$ -subunit has given evidence that these two subunits rotate jointly within the  $\alpha_3\beta_3$  barrel [9–11]. Experiments with single immobilized F<sub>1</sub> parts have shown movements of the  $\epsilon$ -subunit [12,13]. However, the interpretation of these experimental data is not straight forward, since the  $\epsilon$ -subunit is involved not only in the catalytic reaction but also in the activation of the enzyme.

## 2. Single-molecule fluorescence resonance energy transfer

Utilizing single-molecule fluorescence detection [14–16], we have developed a method which allows the observation of subunit movements in membrane-integrated H<sup>+</sup>-ATPsynthases during catalysis [17–20]. This method is based on fluorescence resonance energy transfer (FRET) between two fluorophores, which were covalently bound to the enzyme. According to the

\* Corresponding author.

E-mail address: [peter.graeber@physchem.uni-freiburg.de](mailto:peter.graeber@physchem.uni-freiburg.de) (P. Gräber).

Förster theory, the efficiency of energy transfer depends strongly on the distance between the fluorophores [21]. The FRET efficiency,  $E_{\text{FRET}}$ , can be measured by the fluorescence intensities of the donor ( $F_{\text{D}}$ ) and acceptor ( $F_{\text{A}}$ ).

$$E_{\text{FRET}} = \frac{F_{\text{A}}}{F_{\text{A}} + \gamma F_{\text{D}}} = \frac{R_0^6}{R_0^6 + r_{\text{DA}}^6}, \quad \gamma = \frac{\eta_{\text{A}} \phi_{\text{A}}}{\eta_{\text{D}} \phi_{\text{D}}} \quad (1)$$

with the Förster radius  $R_0$ ; the distance between donor and acceptor  $r_{\text{DA}}$ ; the correction factor  $\gamma$ , with the detection efficiency of photons in the acceptor and donor channel  $\eta_{\text{A}}$  and  $\eta_{\text{D}}$ , and the quantum yield of acceptor and donor  $\phi_{\text{A}}$  and  $\phi_{\text{D}}$ , respectively.

We have built a confocal microscope which allows the detection of fluorescence photons from the donor and acceptor fluorophores with single-molecule sensitivity [17]. This apparatus is shown schematically in Fig. 1, left. The laser beam is focussed in a droplet of buffer (80  $\mu\text{L}$ ) on a microscope cover slide. In our set up a confocal volume of 7 fL is obtained (yellow region in Fig. 1, centre). The fluorophore concentration was adjusted to about 70 pM, so that the average number of fluorophores in the confocal volume was 0.3. The fluorescence intensities in the donor and acceptor channels were recorded simultaneously with avalanche photodiodes (APD) using appropriate filters. The diffusion of the fluorophore through the confocal volume resulted in the detection of a large number of emitted photons during the transit time. From the fluorescence intensities of donor and acceptor, the FRET efficiency was calculated. Fig. 1, centre shows the confocal volume with one trajectory of the diffusing fluorescence labelled enzyme.

The number of fluorescence photons detected by the avalanche photodiode in our set up can be estimated as follows. The power of the Nd/YAG laser (wavelength 532 nm) was adjusted to 120  $\mu\text{W}$  and the laser beam is focussed diffraction limited to an area of  $A = 0.9 \cdot 10^{-12} \text{ m}^2$  (plane with the smallest diameter of the green intensity distribution in Fig. 1, centre).

From the resulting light intensity,  $I$ , the number of photons,  $dN$ , per time,  $dt$ , in this area is calculated.

$$\begin{aligned} I &= \frac{\text{energy}}{\text{time} \cdot \text{area}} = \frac{dQ}{dt \cdot A} = \frac{1.2 \cdot 10^{-4} \text{ W}}{0.9 \cdot 10^{-12} \text{ m}^2} = 1.3 \cdot 10^8 \text{ Wm}^{-2} \\ &= \frac{\text{number of photons} \cdot \text{energy of photon}}{\text{time} \cdot \text{area}} \\ &= \frac{dN \cdot h\nu}{dt \cdot A} \Rightarrow \frac{dN}{dt \cdot A} = \frac{I}{h\nu} = \frac{I \cdot \lambda}{hc} \\ &= \frac{1.3 \cdot 10^8 \text{ Wm}^{-2} \cdot 532 \cdot 10^{-9} \text{ m}}{6.6 \cdot 10^{-34} \text{ Js} \cdot 3 \cdot 10^8 \text{ ms}^{-1}} = 3.5 \cdot 10^{26} \text{ m}^{-2} \text{ s}^{-1} \quad (2) \end{aligned}$$

From the absorption coefficient of TMR at 532 nm ( $\epsilon(532 \text{ nm, TMR}) = 51200 \text{ M}^{-1} \text{ cm}^{-1} = 5120 \text{ m}^2 \text{ mol}^{-1}$ ), the absorption coefficient of one TMR molecule  $\epsilon(1)$  is calculated.

$$\epsilon(1) = \frac{\epsilon(532 \text{ nm, TMR})}{N_{\text{A}}} = \frac{5120 \text{ m}^2 \text{ mol}^{-1}}{6 \cdot 10^{23} \text{ mol}^{-1}} = 8.5 \cdot 10^{-21} \text{ m}^2 \quad (3)$$

The number of photons per time absorbed by one TMR molecule in the focal plane is then

$$\begin{aligned} \frac{dN(\text{abs})}{dt} &= \epsilon(1) \cdot I = 8.5 \cdot 10^{-21} \text{ m}^2 \cdot 3.5 \cdot 10^{26} \text{ m}^{-2} \text{ s}^{-1} \\ &= 3 \cdot 10^6 \text{ s}^{-1} \quad (4) \end{aligned}$$

With the fluorescence quantum yield of the protein bound TMR,  $\phi_{\text{D}} = 0.4$  the number of emitted photons per time is given by

$$\frac{dN(\text{em})}{dt} = \phi_{\text{D}} \frac{dN(\text{abs})}{dt} = 0.4 \cdot 3 \cdot 10^6 \text{ s}^{-1} = 1.2 \cdot 10^6 \text{ s}^{-1} \quad (5)$$

The fluorescence is emitted isotropically in space, the microscope objective collects only those emitted into its direction

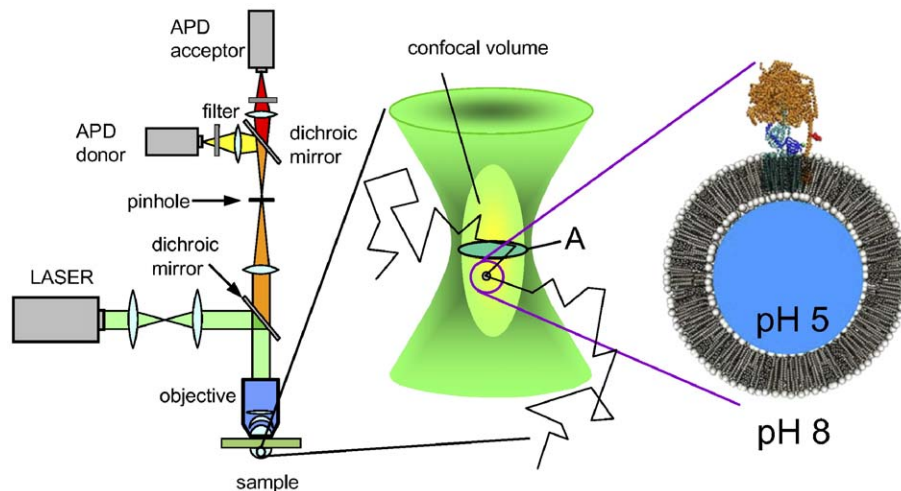


Fig. 1. Scheme of single-molecule fluorescence measurements with fluorescence labelled  $\text{H}^+$ -ATPsynthase from *E. coli* in liposomes. Left, scheme of the confocal apparatus for simultaneous detection of fluorescence from two fluorophores (APD, avalanche photodiode). Centre, trajectory of a liposome through the confocal volume. The intensity distribution of the focussed laser beam is shown in green, the detection volume (due to pinhole) is shown in yellow. The plane of highest light intensity is indicated by the green area (A). Right, fluorescence labelled  $\text{F}_0\text{F}_1$  incorporated into the liposome membrane, with the FRET acceptor (red) at b64, and the FRET donor (green) at  $\epsilon 56$ . A transmembrane pH-difference ( $\text{pH}_{\text{in}} = 5$ ,  $\text{pH}_{\text{out}} = 8$ ) is generated by an acid–base transition.

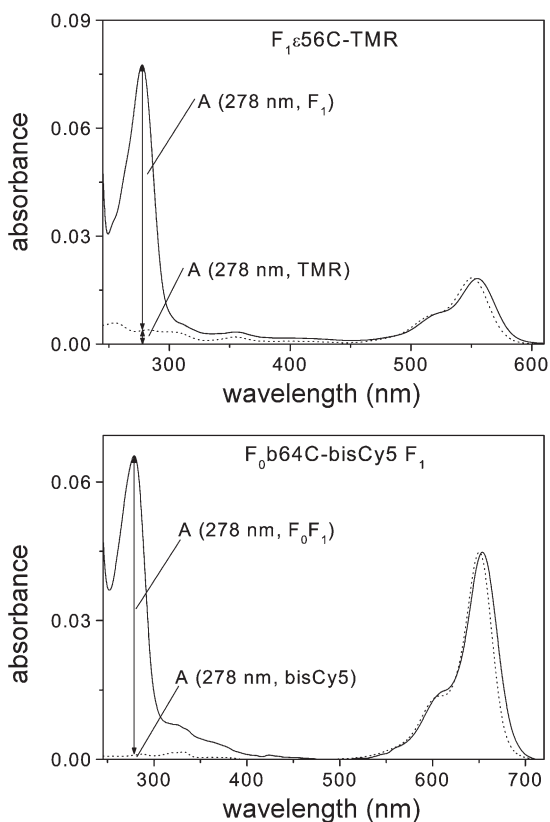


Fig. 2. Absorbance spectra of fluorescence labelled enzymes used for the determination of the labelling degree and the correction of the fluorophore absorbance at 278 nm. Top,  $F_1$  labelled with tetramethylrhodamine (TMR) at  $\epsilon 56$  (solid line), and TMR in buffer (dotted line). Bottom,  $F_0F_1$  labelled with bisCy5 at b64 (solid line), and bisCy5 in buffer (dotted line).

and in addition some photons are lost at the dichroic mirrors and the filters and the APD. This resulted in an overall detection efficiency of our optical set up of  $D=0.08$  and we obtain for the number of detected photons per time.

$$\frac{dN(\text{det})}{dt} = D \cdot \frac{dN(\text{em})}{dt} = 0.08 \cdot 1.2 \cdot 10^6 \text{ s}^{-1} \approx 1 \cdot 10^5 \text{ s}^{-1} \quad (6)$$

We usually measure the fluorescence intensity using the number of photons per ms, i.e., the expected detected fluorescence intensity is 100 photons per ms. This estimation is in accordance with the data measured in this work (see Figs. 3 and 5).

### 3. Biochemical characterization of fluorescence labelled $F_0F_1$

The donor/acceptor labelled  $H^+$ -ATP synthase was constructed as follows. As the site for the acceptor fluorophore we choose that region in the peripheral stalk which is located between the membrane and the  $F_1$  part. For attachment of a fluorescence label, a cysteine was genetically introduced at b64. Since there are two b-subunits in  $F_0F_1$ , we used a Cy5 with two maleimide groups (bisCy5) for fluorescence labelling. BisCy5 maleimide reacts with the cysteines in both b-subunits and cross-links them. Since the fluorophore is attached to the enzyme by two covalent bonds, it has a well-defined position. The

peripheral stalk is part of the stator  $\alpha_3\beta_3\delta ab_2$  of the enzyme. Therefore, the second fluorophore was attached to one of the rotor subunits. We used either the mutant  $\gamma T106C$  and labelled it covalently with the fluorescence donor TMR-maleimide or the  $\epsilon$ -subunit (mutant  $\epsilon H56C$ ), which is involved in catalysis and in activation of the enzyme. To obtain a selective double labelling of the enzyme we used the following procedure [18,19]:

- *E. coli* cells with the mutant bQ64C were grown, and  $F_0F_1$  was isolated.
- $F_0$ -bQ64C- $F_1$  was labelled with bisCy5-maleimide.
- $F_0$ -bQ64C-bisCy5- $F_1$  was reconstituted into liposomes.
- $F_1$  was removed yielding liposomes with membrane-integrated  $F_0$ -bQ64C-bisCy5.
- *E. coli* cells with the mutant  $\gamma T106C$  (or the mutant  $\epsilon H56C$ ) were grown, and the  $F_1$  parts were isolated.
- $F_1$ - $\gamma T106C$  (or  $F_1$ - $\epsilon H56C$ ) was labelled with TMR-maleimide.
- The labelled  $F_1$  part was bound to the liposome-integrated  $F_0$  part leading to  $F_0$ -bQ64C-bisCy5- $F_1^*$ - $\gamma T106C$ -TMR (or  $F_0$ -bQ64C-bisCy5- $F_1^*$ - $\epsilon H56C$ -TMR) (see Fig. 1, right).  $F_1^*$  indicates that this is not the original  $F_1$  part bound to  $F_0$ , but a new  $F_1$  part rebound to  $F_0$ .

The labelled enzymes were characterized by their absorbance spectra, SDS-gel electrophoresis, and by measurement of the rates of ATP synthesis and ATP hydrolysis.

Fig. 2 shows the absorbance spectra of  $F_1$ - $\epsilon H56C$ -TMR and the fluorophore TMR (top), and those of  $F_0$ -bQ64C-bisCy5- $F_1$  and bisCy5 (bottom). From these data, the labelling degree of the enzyme was calculated using the following absorption coefficients,  $\epsilon(278 \text{ nm}, F_0F_1) = 340\,000 \text{ M}^{-1} \text{ cm}^{-1}$ ,  $\epsilon(278 \text{ nm}, F_1) = 204\,000 \text{ M}^{-1} \text{ cm}^{-1}$  [22],  $\epsilon(555 \text{ nm}, \text{TMR}) = 95\,000 \text{ M}^{-1} \text{ cm}^{-1}$ ,  $\epsilon(278 \text{ nm}, \text{TMR}) = 19\,500 \text{ M}^{-1} \text{ cm}^{-1}$ ,  $\epsilon(650 \text{ nm}, \text{bisCy5}) = 250\,000 \text{ M}^{-1} \text{ cm}^{-1}$ ,  $\epsilon(278 \text{ nm}, \text{bisCy5}) = 5\,000 \text{ M}^{-1} \text{ cm}^{-1}$ .

The labelling degree, LD, is calculated from  $LD = [\text{fluorophore}]/[\text{protein}]$ . TMR and bisCy5 also show an absorbance at 278 nm, where the absorbance of the protein is measured. To correct this, the absorbance of the fluorophore at 278 nm is calculated from that at 555 nm (TMR) or 650 nm (bisCy5) according to

$$A(278 \text{ nm}, \text{TMR}) = \frac{\epsilon(278 \text{ nm}, \text{TMR})}{\epsilon(555 \text{ nm}, \text{TMR})} A(555 \text{ nm}, \text{TMR}) \quad (7)$$

The absorbance of the protein is obtained from  $A(278 \text{ nm}, F_1) = A(278 \text{ nm}, \text{measured}) - A(278 \text{ nm}, \text{TMR})$  as indicated in Fig. 2. It should be mentioned that there is a small red shift upon binding of the fluorophores to the protein (see Fig. 2), which has been neglected.

From the data of Fig. 2, the labelling degree of  $F_1$   $LD(\text{TMR}, F_1) = 0.5$ ; the corresponding labelling degree of  $F_0F_1$  was  $LD(\text{bisCy5}, F_0F_1) = 0.94$ . To detect the influence of labelling on enzyme activity, the rates of ATP synthesis and ATP hydrolysis were measured (see Table 1). Comparison of line 1 and 2 shows that labelling of the b-subunit ( $LD = 0.94$ ) slightly decreased the enzyme activity. Removal of  $F_1$  from the membrane-integrated  $F_0F_1$  abolished the enzyme activity completely (line 3 and 4). Rebinding of unlabelled  $F_1$  (line 5)

Table 1

ATP hydrolysis and ATP synthesis rates of the different enzyme preparations at 23 °C. ATP hydrolysis was measured in presence of 1 mM ATP, ATP synthesis in presence of 100  $\mu$ M ADP and 5 mM phosphate after generation of a transmembrane pH difference ( $\text{pH}_{\text{out}}=8.8$ ,  $\text{pH}_{\text{in}}=4.7$ ) and a transmembrane electric potential difference ( $\approx 100$  mV)

Sample	ATP hydrolysis $A_H$ ( $\text{s}^{-1}$ )	ATP synthesis $A_S$ ( $\text{s}^{-1}$ )
1 $F_0\text{b64}F_1$	$71 \pm 4$	$60 \pm 1$
2 $F_0\text{b64-bisCy5 } F_1$	$64 \pm 9$	$48 \pm 1$
3 $F_0\text{b64}$	0	0
4 $F_0\text{b64-bisCy5}$	0	0
5 $F_0\text{b64}F_1^*\epsilon 56$	$55 \pm 8$	$22 \pm 3$
6 $F_0\text{b64-bisCy5}F_1^*\epsilon 56$	$55 \pm 9$	$21 \pm 3$
7 $F_0\text{b64}F_1^*\epsilon 56\text{-TMR}$	$52 \pm 8$	$23 \pm 3$
8 $F_0\text{b64-bisCy5}F_1^*\epsilon 56\text{-TMR}$	$57 \pm 19$	$21 \pm 4$

or labelled  $F_1$  (line 7) to membrane-integrated unlabelled  $F_0$  (line 6) or labelled  $F_0$  (line 8) restored the enzyme activity for all conditions to the same extent.

The rates measured after labelling and rebinding of  $F_1$  referred to samples with several enzyme species. If e.g. the activity of the sample  $F_0$  b64-bisCy5- $F_1^*$ -TMR (line 8) is measured, we had actually the following species in the buffer:  $F_0$  b64  $F_1^*$  (line 5),  $F_0$  b64-bisCy5  $F_1^*$  (line 6),  $F_0$  b64  $F_1^*$   $\epsilon 56$ -TMR (line 7),  $F_0$  b64-bisCy5  $F_1^*$ -TMR (line 8). The species without rebound  $F_1$  do not contribute to the catalytic activity. Since the measured activities of the samples after rebinding of either labelled or unlabelled  $F_1$  to labelled or unlabelled  $F_0$  are, within error limits, identical (see line 5, 6, 7, 8 in Table 1) we conclude that the labelling does not influence significantly the specific activity of the different species.

#### 4. Single-molecule FRET during ATP synthesis and ATP hydrolysis

The double labelled membrane-integrated enzymes ( $F_0$ -bQ64C-bisCy5- $F_1$ - $\epsilon$ H56C-TMR or  $\gamma$ T106C-TMR) have been used to detect the relative subunit movements during catalysis. The liposomes containing not more than one  $F_0F_1$  per liposome were

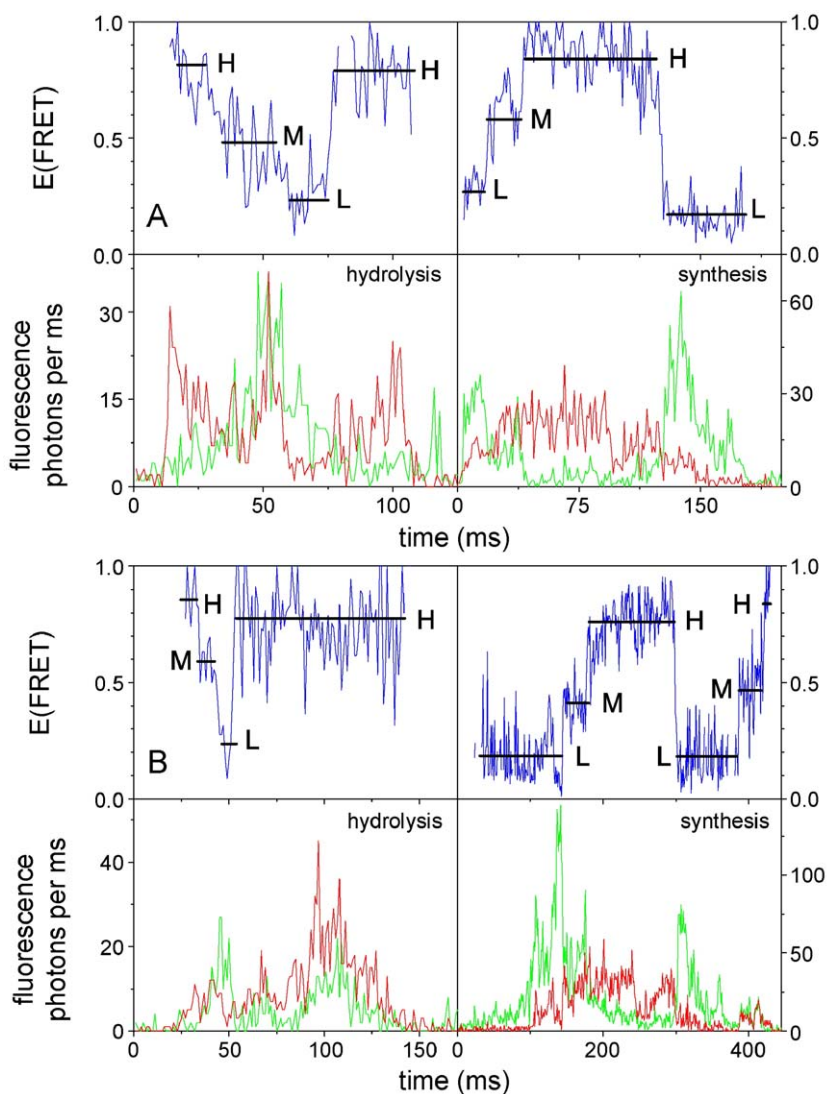


Fig. 3. Fluorescence intensities of FRET donor ( $F_D$ , green), FRET acceptor ( $F_A$ , red) and the calculated FRET efficiencies ( $E_{\text{FRET}}$ , blue). The acceptor (bisCy5) is located in all cases at the b-subunits; the donor (TMR) is located either at the  $\gamma$ -subunit (A) or at the  $\epsilon$ -subunit (B). Left, photon bursts during ATP hydrolysis; right, photon bursts during ATP synthesis.

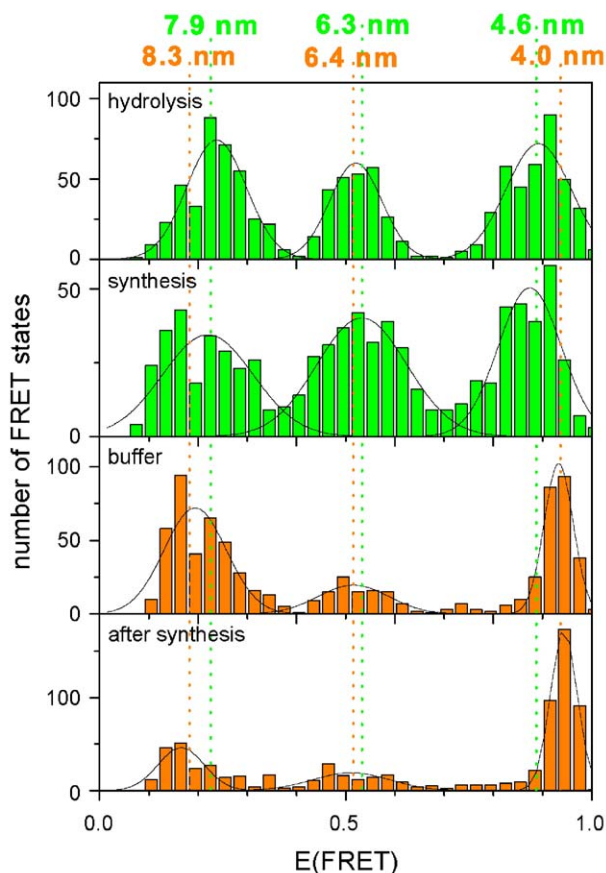


Fig. 4. Histograms of the FRET levels for the active  $F_0F_1$  during catalysis, ATP hydrolysis and ATP synthesis (green), and for the inactive  $F_0F_1$  in buffer without nucleotides and after ATP synthesis (orange). At the top, the distances between  $\epsilon$ -56C-TMR and b64C-bisCy5 are shown as calculated with Eq. (1) from the maxima of the Gaussian distributions.

diluted to 70 pM. When a proteoliposome diffused through the confocal volume (yellow region in Fig. 1, centre), fluorescence from the donor and acceptor was observed. Such an event is called a photon burst. The duration of a burst is between 5 ms and several hundred ms. The fluctuation of the measured fluorescence intensities of donor (green) and acceptor (red) during the burst resulted from the light intensity distribution (see Fig. 1, centre) in the confocal volume. Due to the random diffusion the labelled molecule experiences different excitation light intensities. In addition, the distances between the donor and acceptor can change leading to anticorrelated fluorescence changes of both fluorophores. To separate both effects either the ratio of donor to acceptor fluorescence [18] or the FRET efficiency (Eq. (1)) is calculated. The FRET efficiency is independent of the localization of the double labelled enzyme in the confocal volume and depends on the intramolecular distances, the relative orientation and the microenvironment of the fluorophores. This allows us to measure intramolecular conformational changes in freely diffusing membrane-integrated enzymes. The main advantage of this method is the use of small fluorophores as markers which do not impair the activity of the enzyme. This allows to investigate the membrane-integrated enzyme and to measure ATP synthesis activity after energization of the mem-

brane. A problem is the limited signal to noise ratio, the limited observation time of a diffusing liposome and the bleaching of the fluorophores. The FRET efficiencies and the distances were calculated from the fluorescence intensities of the donor and acceptor using Eq. (1).

Within a photon burst, the FRET efficiency was calculated for each millisecond. The FRET levels were defined as follows: A FRET level was recognized as such when the FRET efficiency was constant for longer than 4 ms and the deviation from the mean was less than 0.15. The average FRET values are shown by black lines in Figs. 3 and 5. All FRET levels were collected in histograms (see Fig. 4). These FRET level histograms can be described by three Gaussian distributions which are called L, M and H.

Fig. 3 shows some fluorescence bursts ( $F_A$ , red and  $F_D$ , green) and the FRET efficiencies (blue) during ATP hydrolysis (left) and ATP synthesis (right). At the top, the data from the labelled  $\gamma$ -subunit ( $F_0$ -bQ64C-bisCy5- $F_1$ - $\gamma$ T106C-TMR) are shown, and at the bottom, those from the labelled  $\epsilon$ -subunit ( $F_0$ -bQ64C-bisCy5- $F_1$ - $\epsilon$ H56C-TMR) are shown. The FRET efficiencies of the  $\gamma$ -labelled enzyme changed in the sequence  $H \rightarrow M \rightarrow L \rightarrow H \dots$  during hydrolysis, and in the opposite sequence  $L \rightarrow M \rightarrow H \rightarrow L \dots$  during ATP synthesis. The same behaviour is observed with the  $\epsilon$ -labelled enzyme. In Fig. 4 top (green), the statistics of the FRET data of the sample  $F_0$ -bQ64C-bisCy5- $F_1$ - $\epsilon$ H56C-TMR from catalytic active bursts (as in Fig. 3B) are shown. The number of FRET levels with a defined FRET efficiency is plotted versus the FRET efficiency. The data show three peaks, which could be attributed to the three FRET levels L, M and H, each one can be described by a Gaussian distribution.

Under non-catalytic conditions, i.e., in the absence of ATP or without energization the photon bursts do not show fluctuations, but a single constant FRET level. Fig. 4 bottom (orange) shows the statistics of the FRET levels observed in buffer pH 8 without nucleotides and after ATP synthesis, when the  $\Delta$ pH has decreased to zero. Again three peaks are observed. The distances between  $\epsilon$ -56C-TMR and b64C-bisCy5 calculated from Eq. (1) are shown at the top of Fig. 4 for catalytic (green) and non-catalytic (orange) conditions. Obviously, the maxima of the Gaussian distributions in the L- and H-state are shifted. The  $\epsilon$ -subunit plays a peculiar role in regulation of the enzyme activity [23]. Our data show that the transition between the active and inactive state is accompanied by a movement of the  $\epsilon$ -56 region within  $F_0F_1$ . The histograms in Fig. 4 indicate that during catalysis (green) the three FRET levels ( $\epsilon$ -b distances) are equally populated. When the enzyme is inactive (resting state) in buffer without nucleotides mostly the high and low FRET levels are populated, after ATP synthesis mostly the high FRET level is populated. Obviously, after ATP synthesis the  $\gamma$ - $\epsilon$  complex is not docked arbitrarily to one  $\alpha\beta$  pair, it stops at that pair, which is characterized by the lowest  $\epsilon$ -56/b64-distance, i.e., this state must have a lower Gibbs free energy than the two others.

From the maxima of the Gaussian distribution the distances are calculated from Eq. (1) with  $\gamma=0.87$  and  $R_0=6.4$  nm for  $\epsilon$ H56C-TMR and  $\gamma=0.94$  and  $R_0=6.3$  nm for  $\gamma$ T106C-TMR. The results are collected in Table 2.

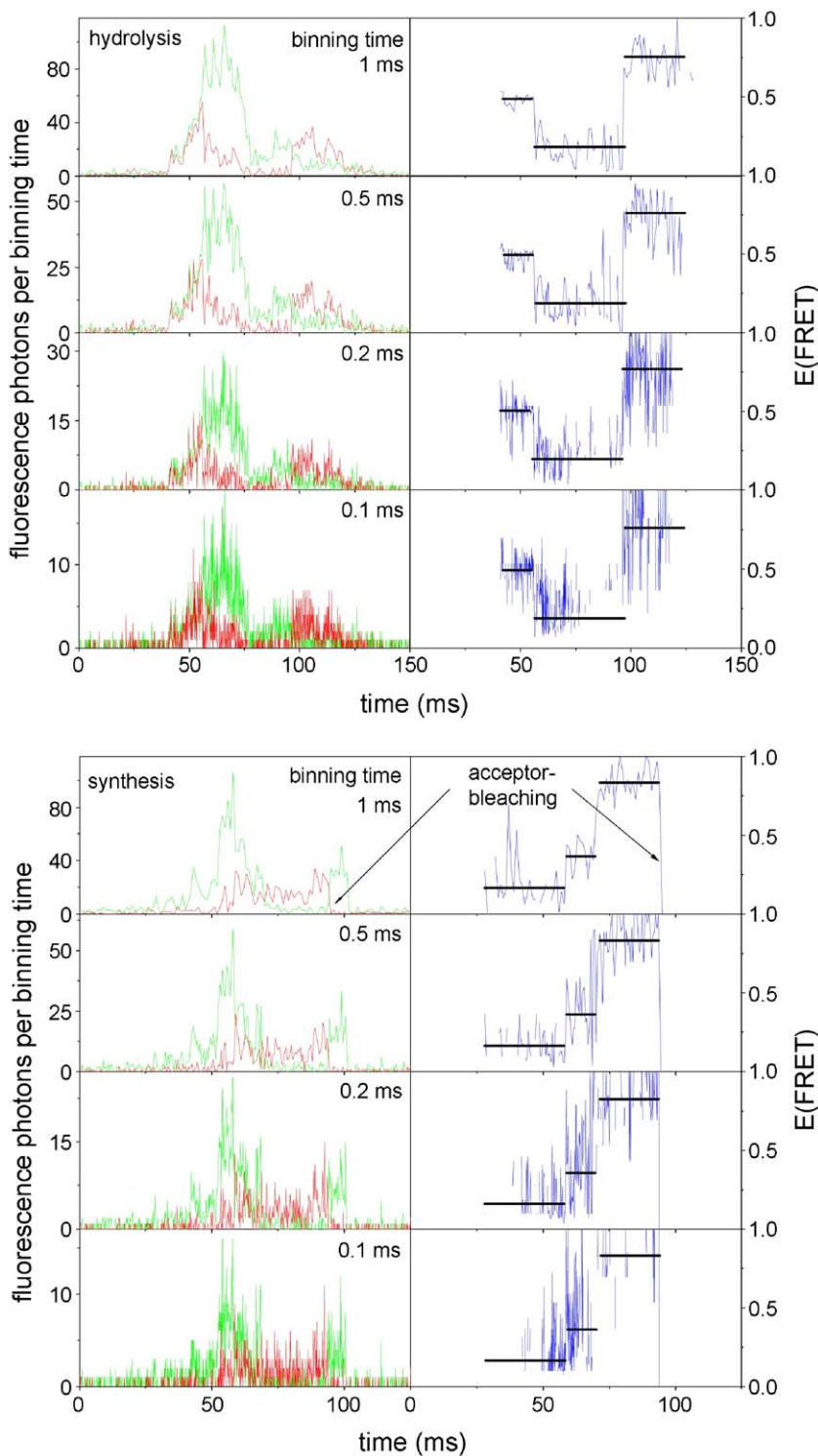


Fig. 5. Photon bursts and FRET efficiencies at different time resolutions with TMR at the  $\epsilon$ -subunit. The binning time was varied between 1 ms and 0.1 ms. ATP hydrolysis is shown at the top, ATP synthesis at the bottom. In the ATP synthesis trajectory photo bleaching of the acceptor fluorophore is observed at 96 ms.

The three distances calculated from the FRET data and those obtained from the homology model are similar and we conclude that the movement of the  $\gamma$ - and the  $\epsilon$ -subunit relative to the b-subunit during ATP hydrolysis in the membrane-integrated  $F_0F_1$  can be described by a  $120^\circ$  stepwise rotation around an axis in the centre of the  $\alpha_3\beta_3$  barrel. This is consistent with earlier data on the

rotation of  $\gamma$  in  $F_1$  [5,6]. In addition our data show, at first, that rotation of  $\gamma$  and  $\epsilon$  occurs also during ATP synthesis, i.e., under conditions, where the catalytic reaction in  $F_1$  is coupled with proton translocation through  $F_0$  and secondly, that rotation during ATP synthesis occurs in the opposite direction as during ATP hydrolysis. It should be mentioned that for the estimation of the

Table 2

Distances between b-Q64C-bisCy5 and  $\epsilon$ -H56C-TMR or  $\gamma$ -T106C-TMR calculated from the FRET efficiencies during catalysis, and the corresponding C $\alpha$ –C $\alpha$  distances obtained from the homology model according to three 120° steps around a central axis

	$\gamma$ T106C-TMR			$\epsilon$ H56C-TMR		
	H	M	L	H	M	L
FRET efficiency	0.79±0.07	0.49±0.09	0.22±0.06	0.87±0.07	0.53±0.09	0.21±0.09
Distance (FRET) (nm)	5.1±0.4	6.3±0.4	7.8±0.5	4.6±0.5	6.3±0.4	7.9±0.7
C $\alpha$ –C $\alpha$ distance in homology model (nm)	5.0	7.3	8.5	4.2	5.1	8.3

distances from the FRET data, we use the approximation that the orientation factor  $\kappa^2=2/3$ . This is correct only for an unrestricted rotational movement of the fluorophores. For the estimation of the distances from the homology model, we use the approximation that the position of the b-subunits does not change during catalysis. In view of these approximations, the coincidence between these completely independent approaches is surprising.

The movement of the  $\gamma$ - and the  $\epsilon$ -subunit during catalysis is not a smooth, continuous rotation but a stepped movement. The FRET efficiency, i.e., the distance between the donor at the  $\gamma$ - or the  $\epsilon$ -subunit and the acceptor at the b-subunits of the peripheral stalk, remained constant up to several hundred ms, and then rapidly changed within 1 ms, the time resolution of the measurement, to the next FRET level (see Fig. 3). The time interval of constant FRET efficiency is called the “dwell time” and this is interpreted as the docking time of the  $\gamma$ -subunit to one  $\alpha\beta$  pair. The undocking/docking step to the next  $\alpha\beta$  pair was faster than 1 ms. The average dwell times during ATP synthesis (and ATP hydrolysis) are collected in Table 3, together with the turnover times,  $\tau$ , calculated from the activity, A, of the biochemical ensemble of the labelled enzymes (line 8, Table 1),  $\tau=1/A$ .

Since the average dwell times calculated from the single-molecule experiments are in accordance with the average turnover times for synthesis (or hydrolysis) of one ATP per enzyme obtained from the biochemical ensemble measurements, we conclude, that the dwell times represent the time for synthesis (or hydrolysis) of one ATP at a specific  $\alpha\beta$  pair. The data in Fig. 3 show that there is a large variability in the dwell times and this implies that the time for synthesis (or hydrolysis) of one ATP can vary considerably. According to the binding change theory, different steps of the catalytic reaction take place

Table 3

Average dwell times during ATP synthesis and ATP hydrolysis obtained from single-molecule FRET with  $F_0$ -bQ64C-bisCy5- $F_1^+$ - $\gamma$ T106C-TMR and  $F_0$ -bQ64C-bisCy5- $F_1^+$ - $\epsilon$ H56C-TMR and the corresponding turnover times calculated from the rates obtained with ensemble measurements with otherwise identical conditions

	$\gamma$ T106C-TMR		$\epsilon$ H56C-TMR	
	ATP synthesis	ATP hydrolysis	ATP synthesis	ATP hydrolysis
Rate from ensemble measurement ( $s^{-1}$ )	23	67	21	57
Turnover time from ensemble measurement (ms)	43	15	48	18
Average dwell time from single-molecule measurement (ms)	51	19	18	14

simultaneously at the catalytic site of each  $\alpha\beta$  pair, that is, binding of substrate at site 1 (“open site”), catalysis at site 2 (“tight site”), and release of products at site 3 (“loose site”). The movement of the  $\gamma$ -subunit has been resolved into several substeps (ATP binding, reaction, product release) [8]. We have not yet been able to observe such substeps with FRET.

During the dwell time, the distance between the labelled rotor subunits and the b-subunits did not change, and it might be asked, how fast is the undocking/docking process (switch from one to the next  $\alpha\beta$  pair). For the measurement of the photon bursts in Fig. 3, a time resolution (“binning time”) of 1 ms was used, that is, the photons arriving in 1 ms were accumulated. To show the effect of binning time on the signal to noise ratio of donor and acceptor fluorescence and on the FRET efficiency photon bursts were measured with a time window of 0.1 ms. The data with lower time resolution (0.2, 0.5 and 1 ms) were calculated by summing up the 0.1 ms time bins.

Fig. 5 shows the same photon bursts one during ATP synthesis (bottom) and ATP hydrolysis (top) displayed with time windows between 0.1–1 ms. The data show an increasing signal to noise ratio with increasing binning time. The average FRET efficiency during each dwell time remained at the same level independent of the time resolution (black lines). It should be noted, that, by coincidence, photo bleaching of the acceptor can be seen in the photon burst during ATP synthesis (see Fig. 5, bottom). Such an event shows unequivocally that only one molecule of the acceptor fluorophore was present in the

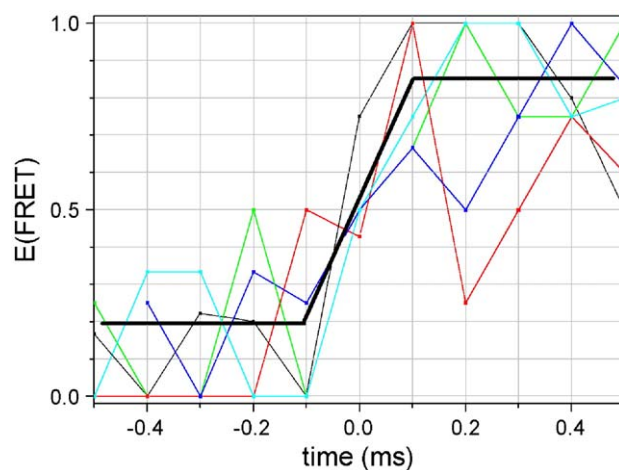


Fig. 6. Superposition of the FRET efficiency changes of the L→H transitions from five photon bursts with TMR at the  $\epsilon$ -subunit. Five L→H transitions with a binning time of 0.1 ms are superposed. The average FRET level of the signals is indicated by a black solid line.

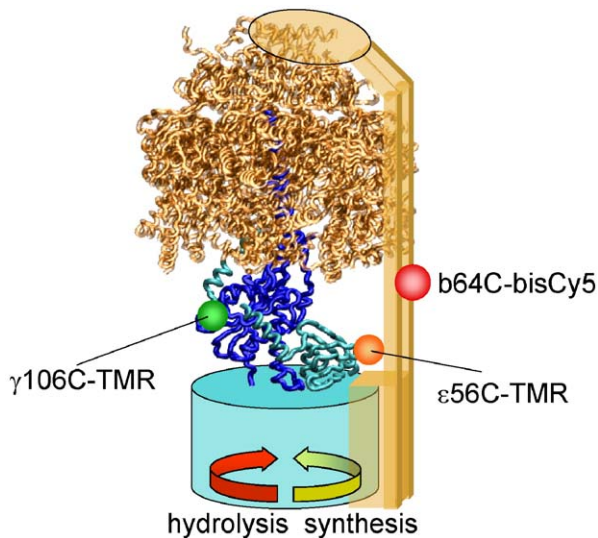


Fig. 7. Patchwork model of the  $H^+$ -ATP synthase from *E. coli* with the positions of  $\epsilon 56$  (orange),  $\gamma 106$  (green) and  $b64$  (red). Arrows indicate direction of rotation.

confocal volume. In addition, the kinetics of the photon bleaching indicated that this process occurs faster than our time resolution of 0.1 ms. The signal to noise ratio of the data in Fig. 5 did not allow an appropriate calculation of the reaction time of the FRET transition. To get an estimation of this time, we superposed the data from five  $L \rightarrow H$  transitions during ATP hydrolysis with the highest time resolution in Fig. 6. The black line shows the average of these five experiments and we can estimate that the reaction time is faster than 0.2 ms for the undocking/docking process. These data revealed a very peculiar movement of the  $\gamma$ - $\epsilon$  complex relative to the b-subunits during ATP synthesis and ATP hydrolysis: Waiting time intervals (dwell times up to hundred ms) were followed by rapid movements (reaction time shorter than 0.2 ms), and followed again by waiting time intervals. Such a stepped motion had been proposed earlier on the basis of spectroscopic ensemble measurements with immobilized  $CF_1$  [24] and has been observed directly with the immobilized thermophilic  $F_1$  [7]. The analysis of the movement of a gold bead attached to  $F_1$  has revealed a similar transition time as described here [8]. Our data show that such a stepped motion is also observed during proton transport-coupled catalysis in the membrane-integrated holoenzyme. The location of the donor fluorophore at the  $\gamma$ - or  $\epsilon$ -subunit and that of the acceptor at the b-subunit is shown in the model in Fig. 7. The directions of rotation during ATP hydrolysis and ATP synthesis are indicated. What happens during the waiting time on the catalytic nucleotide binding sites and how the movement of the  $\gamma$ - $\epsilon$  complex is coupled to the c-ring rotation remains to be clarified.

## Acknowledgements

We thank R. A. Capaldi and R. Aggeler for the gift of the  $\gamma T106C$  mutant, C.A.M. Seidel for the gift of bisCy5. This work was financially supported by the Graduiertenkolleg

“Biochemie der Enzyme” and by the Landesstiftung Baden-Württemberg, Projekt “Functional Nanodevices”.

## References

- [1] A.E. Senior, S. Nadanaciva, J. Weber, The molecular mechanism of ATP synthesis by  $F_1F_0$ -ATP synthase, *Biochim. Biophys. Acta* 1553 (2002) 188–211.
- [2] P.D. Boyer, The binding change mechanism for ATP synthase—Some probabilities and possibilities, *Biochim. Biophys. Acta* 1140 (1993) 215–250.
- [3] T.M. Duncan, V.V. Bulygin, Y. Zhou, M.L. Hutcheon, R.L. Cross, Rotation of subunits during catalysis by *Escherichia coli*  $F_1$ -ATPase, *Proc. Natl. Acad. Sci. U. S. A.* 92 (1995) 10964–10968.
- [4] D. Sabbert, S. Engelbrecht, W. Junge, Intersubunit rotation in active  $F_1$ -ATPase, *Nature* 381 (1996) 623–625.
- [5] Y. Zhou, T.M. Duncan, R.L. Cross, Subunit rotation in *Escherichia coli*  $F_0F_1$ -ATP synthase during oxidative phosphorylation, *Proc. Natl. Acad. Sci. U. S. A.* 94 (1997) 10583–10587.
- [6] G. Kaim, M. Prummer, B. Sick, G. Zumofen, A. Renn, U.P. Wild, P. Dimroth, Coupled rotation within single  $F_0F_1$  enzyme complexes during ATP synthesis or hydrolysis, *FEBS Lett.* 525 (2002) 156–163.
- [7] H. Noji, R. Yasuda, M. Yoshida, K. Kinosita Jr., Direct observation of the rotation of  $F_1$ -ATPase, *Nature* 386 (1997) 299–302.
- [8] R. Yasuda, H. Noji, M. Yoshida, K. Kinosita Jr., H. Itoh, Resolution of distinct rotational substeps by submillisecond kinetic analysis of  $F_1$ -ATPase, *Nature* 410 (2001) 898–904.
- [9] C. Tang, R.A. Capaldi, Characterization of the interface between  $\gamma$  and  $\epsilon$  subunits of *Escherichia coli*  $F_1$ -ATPase, *J. Biol. Chem.* 271 (1996) 3018–3024.
- [10] R. Aggeler, I. Ogilvie, R.A. Capaldi, Rotation of a  $\gamma$ - $\epsilon$  subunit domain in the *Escherichia coli*  $F_1F_0$ -ATP synthase complex. The  $\gamma$ - $\epsilon$  subunits are essentially randomly distributed relative to the  $\alpha_3\beta_3\delta$  domain in the intact complex, *J. Biol. Chem.* 272 (1997) 19621–19624.
- [11] V.V. Bulygin, T.M. Duncan, R.L. Cross, Rotor/Stator interactions of the  $\epsilon$  subunit in *Escherichia coli* ATP synthase and implications for enzyme regulation, *J. Biol. Chem.* 279 (2004) 35616–35621.
- [12] K. Häslner, S. Engelbrecht, W. Junge, Three-stepped rotation of subunits  $\gamma$  and  $\epsilon$  in single molecules of  $F_1$ -ATPase as revealed by polarized, confocal fluorometry, *FEBS Lett.* 426 (1998) 301–304.
- [13] Y. Kato-Yamada, H. Noji, R. Yasuda, K. Kinosita Jr., M. Yoshida, Direct observation of the rotation of epsilon subunit in  $F_1$ -ATPase, *J. Biol. Chem.* 273 (1998) 19375–19377.
- [14] S. Weiss, Measuring conformational dynamics of biomolecules by single-molecule fluorescence spectroscopy, *Nat. Struct. Mol. Biol.* 7 (2000) 724–729.
- [15] P.J. Rothwell, S. Berger, O. Kensch, S. Felekyan, M. Antonik, B.M. Wöhrl, T. Restle, R.S. Goody, C.A.M. Seidel, Multiparameter single-molecule fluorescence spectroscopy reveals heterogeneity of HIV-1 reverse transcriptase: primer/template complexes, *Proc. Natl. Acad. Sci. U. S. A.* 100 (2003) 1655–1660.
- [16] T. Ha, Single-molecule fluorescence resonance energy transfer, *Methods* 25 (2001) 78–86.
- [17] M. Börsch, M. Diez, B. Zimmermann, R. Reuter, P. Gräber, Stepwise rotation of the  $\gamma$ -subunit of  $EF_0F_1$ -ATP synthase observed by intramolecular single-molecule fluorescence resonance energy transfer, *FEBS Lett.* 527 (2002) 147–152.
- [18] M. Diez, B. Zimmermann, M. Börsch, M. König, E. Schweinberger, S. Steigmiller, R. Reuter, S. Felekyan, V. Kudryavtsev, C.A. Seidel, P. Gräber, Proton-powered subunit rotation in single membrane-bound  $F_0F_1$ -ATP synthase, *Nat. Struct. Mol. Biol.* 11 (2004) 135–141.
- [19] B. Zimmermann, M. Diez, N. Zarrabi, P. Gräber, M. Börsch, Movements of the  $\epsilon$ -subunit during catalysis and activation in single membrane-bound  $H^+$ -ATP synthase, *EMBO J.* 24 (2005) 2053–2063.
- [20] F.-M. Boldt, J. Heinze, M. Diez, J. Petersen, M. Börsch, Real-time pH microscopy down to the molecular level by combined scanning

- electrochemical microscopy/single-molecule fluorescence spectroscopy, *Anal. Chem.* 76 (2004) 3473–3481.
- [21] T. Förster, Zwischenmolekulare Energiewanderung und Fluoreszenz, *Ann. Phys.* 2 (1948) 55–70.
- [22] S.C. Gill, P.H. von Hippel, Calculation of protein extinction coefficients from amino acid sequence data, *Anal. Biochem.* 182 (1989) 319–326.
- [23] S.P. Tsunoda, A.J. Rodgers, R. Aggeler, M.C. Wilce, M. Yoshida, R.A. Capaldi, Large conformational changes of the  $\epsilon$  subunit in the bacterial  $F_1F_0$  ATP synthase provide a ratchet action to regulate this rotary motor enzyme, *Proc. Natl. Acad. Sci. U. S. A.* 98 (2001) 6560–6564.
- [24] D. Sabbert, W. Junge, Stepped versus continuous rotatory motors if the molecular scale, *Proc. Natl. Acad. Sci. U. S. A.* 94 (1997) 2312–2317.